

Optimization and Scale-Up of the Continuous Flow Acetylation and Nitration of 4-Fluoro-2-methoxyaniline to Prepare a Key Building Block of Osimertinib

Manuel Köckinger, Benjamin Wyler, Christof Aellig, Dominique M. Roberge, Christopher A. Hone,* and C. Oliver Kappe*



Cite This: <https://dx.doi.org/10.1021/acs.oprd.0c00254>



Read Online

ACCESS |



Metrics & More



Article Recommendations



Supporting Information

ABSTRACT: The development of a scalable telescoped continuous flow procedure for the acetylation and nitration of 4-fluoro-2-methoxyaniline is described. A subsequent batch deprotection then affords 4-fluoro-2-methoxy-5-nitroaniline, a key building block in the synthesis of osimertinib, a third-generation epidermal growth factor receptor tyrosine kinase inhibitor (EGFR-TKI) that is used for the treatment of nonsmall-cell lung carcinomas carrying EGFR-TKI sensitizing and EGFR T790M resistance mutations. The hazards associated with nitration of organic compounds, such as thermal runaway and explosivity of intermediates, make it difficult to scale up nitrations to industrial quantities, particularly within large-scale batch reactors. In this study, we investigated an acetic acid/aqueous nitric acid mixture as a predominantly kinetically controlled nitration regime and a water-free mixture of acetic acid, fuming nitric acid, and fuming sulfuric acid (oleum) as a mass-transfer-limited nitration regime. A modular microreactor platform with in-line temperature measurement was utilized for the nitration. Furthermore, we identified that it was necessary to protect the amine functionality through acetylation to avoid side reactions. The process parameters and equipment configuration were optimized at laboratory scale for the acetylation and nitration to improve the product yield and purity. The two steps could be successfully telescoped, and the laboratory-scale flow process was operated for 80 min to afford the target molecule in 82% isolated yield over two steps, corresponding to a throughput of 25 mmol/h. The developed flow process was then transferred to an industrial partner for commercial implementation and scaled up by the use of higher flow rates and sizing-up of the microreactor platform to pilot scale to afford the product in 83% isolated yield, corresponding to a throughput of 2 mol/h (0.46 kg/h).

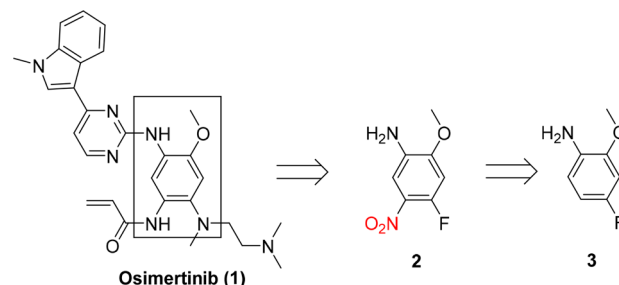
KEYWORDS: continuous flow, nitration, acetylation, osimertinib, modular microreactor platform, scale-up

INTRODUCTION

Osimertinib (**1**) is an active pharmaceutical ingredient (API) developed by AstraZeneca. It is a third-generation, irreversible, oral epidermal growth factor receptor tyrosine kinase inhibitor (EGFR-TKI) that potently and selectively inhibits EGFR-TKI sensitizing and EGFR T790M resistance mutations.^{1–3} The EGFR T790M resistance mutation can be de novo or acquired through previous treatment with first- or second-generation EGFR-TKIs.⁴ Currently, **1** is used as a first-line treatment for patients with locally advanced or metastatic nonsmall-cell lung carcinoma (NSCLC) with EGFR sensitizing mutations and as a treatment for patients with EGFR T790M-mutation-positive NSCLC that has progressed on or after EGFR-TKI therapy.

A core building block in the synthesis of **1** is a tetrasubstituted benzene ring that is derived from 4-fluoro-2-methoxy-5-nitroaniline (**2**) (Scheme 1). Compound **2** can be prepared by the nitration of 4-fluoro-2-methoxyaniline (**3**). According to the patent literature, compound **2** can be synthesized by preparing a 1.13 M solution of aniline **3** in concentrated sulfuric acid (H₂SO₄) at 0 °C. Subsequent treatment with 1 equiv of potassium nitrate (KNO₃) and stirring overnight affords compound **2** in 77% yield after purification by column chromatography.⁵ In a different protocol, a 0.43 M solution of compound **3** in concentrated

Scheme 1. Structure of AstraZeneca's Tyrosine Kinase Inhibitor Osimertinib (1) Synthesized from 4-Fluoro-2-methoxy-5-nitroaniline (2), the Nitration Product of 4-Fluoro-2-methoxyaniline (3)

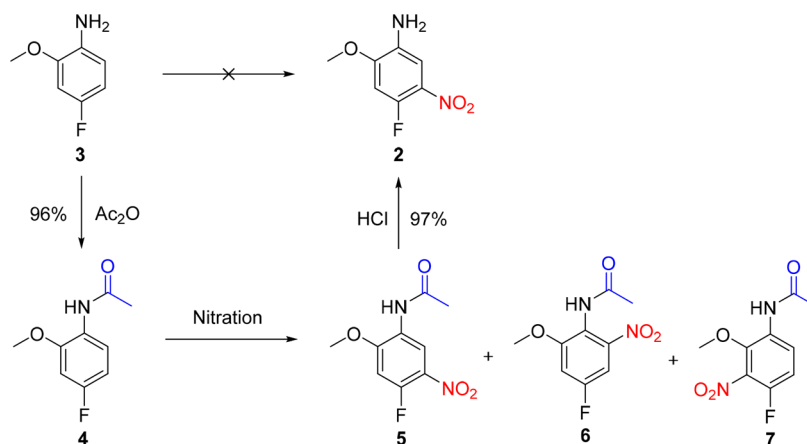


H₂SO₄ was prepared at –20 °C and treated with 1.11 equiv of concentrated nitric acid (HNO₃) to provide compound **2** in

Special Issue: Flow Chemistry Enabling Efficient Synthesis

Received: May 29, 2020



Scheme 2. Protection Group Strategy for the Synthesis of **2** from **3** by Acetylation with Ac_2O ^a

^aRegioisomers **5** and **6** were formed by nitration. Regioisomer **7** could also potentially be formed but was not observed throughout this study.

80% yield without the need for column chromatography.⁶ Synthetic routes to **1** have been discussed in detail elsewhere.⁷ Notably, particular effort has been made to optimize certain steps within a continuous flow environment.⁸

Nitration reactions are inherently dangerous transformations since they are generally highly exothermic and rely on the use of corrosive and sometimes toxic nitration agents.⁹ A key danger is the use of a strongly oxidizing material (HNO_3) in conjunction with reducible substrates. For these reasons, nitration reactions are notoriously difficult to scale up and constitute one of the most hazardous reactions for chemical manufacture.¹⁰ To ensure constant product quality in nitration reactions, precise control over the temperature and reagent stoichiometry should be ensured because small fluctuations can lead to overnitration, oxidation,¹¹ or polymerization.^{10,11} The oxidation side reaction is a key safety issue, especially when the nitration is performed at temperatures above 80 °C.¹¹ The utilization of microreactors has been demonstrated to alleviate the above-mentioned challenges through enhanced heat transfer and improved mixing.¹² In addition, the flow rates can be carefully controlled, which enables the precise addition of reagents. Within a continuous flow reactor, only a small amount of chemical inventory is processed at any one time, which considerably minimizes the risk and potential scale of explosions or thermal runaway. These advantages make continuous processes inherently safer and more controlled than operation within a batch environment, particularly at larger scales.¹³ The application of microreaction technology to perform nitration reactions was reported as early as 1956.¹⁴ Nitration reactions within continuous flow environments have received significant attention since that time, with recent developments encompassing the nitration of important API building blocks.^{10,15,16} In particular, a team from Novartis developed a protocol using fuming nitric acid that resulted in improved safety, higher product quality, and a straightforward scale-up.¹⁰ The continuous flow nitration of benzyl-protected vanillin to *O*-benzyl-6-nitrovanillin on a multikilogram scale has been described by a group at Bristol-Myers Squibb (BMS).¹⁷ The protection of the hydroxyl group provided the desired selectivity for the process and reduced the formation of the undesired 5-nitrovanillin. Subsequently, a batch deprotection with trifluoroacetic acid (TFA) in dichloromethane (DCM) afforded the desired compound 6-nitrovanillin. Our group has previously reported on nitration reactions involving

highly explosive intermediates that were directly hydrogenated in multistep cascaded flow processes.¹⁸

A toolbox approach was devised to facilitate the transfer of chemical reactions from batch to continuous flow processes.¹⁹ In this toolbox approach, chemical reactions are categorized on the basis of their intrinsic reaction rates under conventional operating conditions. Type A reactions are defined as having high reaction rates and reach completion within seconds. These reactions, which occur with half-lives of less than 1 s, are mass-transfer-limited reactions and thus are mixing-controlled. Type B reactions occur on an intermediate time scale with half-lives of seconds to minutes. Type C reactions are relatively slow, on time scales of approximately more than 10 min, but could benefit from transfer to flow to improve safety or quality. Type B and C reactions can be defined as predominantly kinetically controlled. Nitration reactions can fall into all three of these categories.

We were interested in developing a scalable nitration protocol for the synthesis of **2** through the utilization of continuous processing. Our primary focus was on generating data that would enable a smooth scale-up of the process. Different nitration conditions for the transformation were explored, including a nitration with acetic acid and aqueous nitric acid as a predominantly kinetically controlled (type B/C) system and a water-free nitration with acetic acid/fuming sulfuric acid (oleum)/fuming nitric acid as a mass-transfer-limited (type A reaction) system. Herein we describe the optimization of the nitration reaction within continuous flow, the development of a telescoped continuous flow acetylation and nitration procedure, and subsequent technology transfer from laboratory to pilot scale.

RESULTS AND DISCUSSION

In our initial trials, we evaluated existing patent protocols by using concentrated H_2SO_4 and KNO_3 or HNO_3 for the nitration of 4-fluoro-2-methoxyaniline (**3**) at a low temperature.^{5,6} These initial trials resulted in the formation of a heterogeneous mixture that was difficult to stir. The reaction mixture contained only trace amounts of the desired product 4-fluoro-2-methoxy-5-nitroaniline (**2**). Major side products were detected, possibly caused by oxidation of the amino group. These results are different from the reported yields in patent applications.^{5,6} The elevated levels of side product formation can conceivably be explained by the significant

exotherm observed, even with careful addition of the nitration reagents. Using acetic acid (AcOH) and concentrated HNO_3 as an alternative nitration mixture, as presented by Brocklehurst and co-workers on a similar substrate,¹⁰ also resulted in a mixture of side products. As the preliminary investigation of direct nitration approaches failed, we chose to acetylate **3** using acetic anhydride (Ac_2O) to afford acetamide **4** in order to avoid side reactions occurring at the amino functionality (Scheme 2). The acetyl group of compound **5** can be cleaved under batch conditions in nearly quantitative yield by the use of dilute HCl to afford the desired product **2**.

A. Predominantly Kinetically Controlled Nitration.

We next investigated the batch nitration of acetyl-protected **4** with aqueous HNO_3 . For the experiment, a 1 M solution of substrate **4** in AcOH was treated with 30 equiv of concentrated HNO_3 (69 wt %, 15 M), and the resulting mixture was heated in a dedicated microwave reactor at 80 °C for 15 min. The nitration of substrate **4** in AcOH/ HNO_3 can be considered as a type B/C reaction and is predominantly kinetically controlled.¹⁹ The formation of the desired nitration product **5** was observed in 94% yield along with a minor amount (<6% yield) of regioisomer **6** (based on HPLC area %). Regioisomer **6** was highly water-soluble, and thus, separation from the desired isomer was particularly simple. We observed a significant exotherm during the initial batch microwave experiments, so we commenced flow experiments, which would provide better temperature control. In general, the heat of reaction for nitration reactions ranges from -73 to -253 kJ/mol.¹⁵ The translation of batch microwave conditions to conventionally heated continuous flow environments is a well-established technique.²⁰ The heat generated from the exotherm could be far better controlled through the utilization of a continuous flow reactor, and thus, all subsequent nitration experiments were performed using a flow reactor.

We chose to use a Modular MicroReaction System (MMRS) equipped with a FlowPlate Lab (channel width = 2 mm, mixer nominal width = 0.2 mm, volume = 0.4 mL), manufactured by Ehrfeld Mikrotechnik.^{19,21,22} The system has been applied for the successful scale-up of a number of important chemical transformations,^{19,21,22} and it has been successfully demonstrated to withstand corrosive nitration mixtures because of its construction from Hastelloy C22.²³ An overall heat transfer coefficient, U , of ~ 2200 $\text{W m}^{-2} \text{K}^{-1}$ was measured by Mielke et al. for the FlowPlate reactor.^{21d} Additionally, we have previously demonstrated the incorporation of online process analytical tools (PATs) within the MMRS for rapid data acquisition.²²

The two feeds, one for the substrate dissolved in AcOH and the other for the nitric acid solution, were introduced by syringe pumps. A liquid/liquid (LL) mixing plate (Figure 1) was used as an inlay for the FlowPlate to ensure optimal mixing and facile scalability (see section C for more details).²¹ In this study, we incorporated an in-line temperature sensor at the outlet of the plate, and a thermostat (Huber CC 304) was used for temperature control. The temperature change over time was visually observed on the display of the thermostat. The pump rate of the thermostat was set at a sufficient circulation speed to ensure that the changes in the inlet and outlet temperatures of the process fluid did not exceed +1 °C from the set point conditions during the experiments.

We commenced our flow studies by translating the microwave batch conditions to continuous flow. The reaction occurs on the time scale of minutes (type B/C), and thus, a

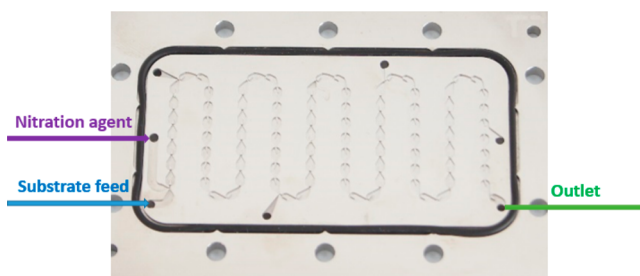
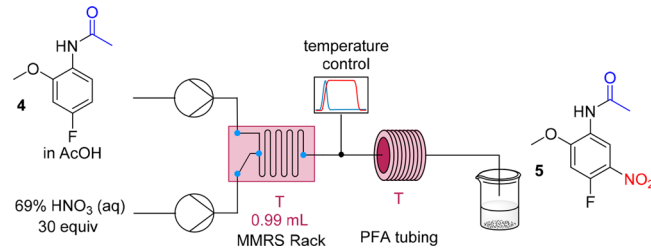


Figure 1. FlowPlate Lab liquid/liquid (LL) mixing plate consisting of seven inlets/outlets and 70 mixing structures. The nitration agent inlet, substrate feed inlet, and reaction outlet used in this study are indicated on the image. The FlowPlate Lab is constructed from Hastelloy C22, and the viewing point was manufactured from Hastelloy C276 and sapphire. The surface area of the plate is 74 mm \times 104 mm.

reactor coil (PFA, $\frac{1}{8}$ in. o.d., 0.8 mm i.d., $V = 7$ mL) was used after the FlowPlate to provide sufficient residence time. The coil was submerged in a water bath for temperature control. Upon transfer to flow, operating at 70 °C with a residence time of 16 min afforded product **5** in 98% yield (Table 1, entry 1). A reduction in the amount of HNO_3 from 30 to 15 equiv resulted in a lower yield of 64% (entry 2). A lower temperature of 20 °C caused only a minor drop in yield to 94%, indicating the weak temperature dependence of the reaction. As we were interested in a protocol that is easy to scale, we were keen on using only the reactor volume of the FlowPlate. Removing the reactor coil resulted in a shorter residence time of 1 min, and a drop in yield to 88% was observed (entry 3). The yield could be increased by heating the reactor to 60 °C. A yield of >99% was obtained within a residence time of 30 s by heating the reactor to 80 °C (entry 7). Product **5** could be isolated in 86% yield after recrystallization. These optimization data show that increasing the reaction temperature can drastically improve the space-time yield because a comparatively small reactor volume can be used. The temperature dependence of the reaction indicated that we were operating within a predominately kinetically controlled regime (entries 4–6). However, at the shortest residence times we were likely to be approaching mass-transfer-limited conditions (entry 7). We concluded that under the identified conditions, the large excess of nitric acid would lead to exacerbated salt waste. We also determined that the aqueous nitric acid would be at the corrosivity limit for the equipment at 80 °C. Therefore, an alternative strategy was sought that used a more reactive nitration system and water-free conditions.

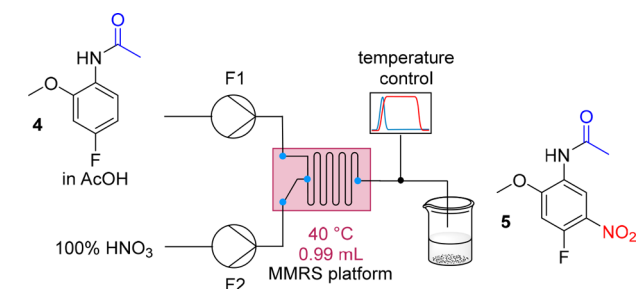
The continuous flow process was reoptimized using white fuming nitric acid (99 wt %) as a replacement for 69% aqueous nitric acid (Scheme 3). Fuming nitric acid is a stronger nitrating agent, but it is usually less corrosive toward most materials.^{10,23} Employing the same reaction conditions as with aqueous nitric acid (Table 1, entry 7) resulted in the formation of a number of side products. Decomposed starting material was observed even when only 1.0 equiv of nitric acid was used. When 69% aqueous nitric acid was used, only very trace amounts of side products were observed. However, in the case of 99 wt % fuming nitric acid, a range of side products formed, comprising of different oxidation products (phenol derivatives) and overnitration products. The temperature was lowered in order to circumvent the formation of those potentially explosive or toxic side products.¹¹ When the temperature of

Table 1. Optimization of the Reaction Conditions for the Nitration of **4** to the Nitrated Analogue **5** Using Aqueous Nitric Acid^a


entry	conc. of 4 within the reactor [M]	reactor volume [mL]	total flow rate [mL/min]	temperature [°C]	residence time [min]	yield [%] ^c
1	0.33	8	0.5	70	16	98
2 ^b	0.50	8	0.5	70	16	64
3	0.33	8	1	20	8	94
4	0.33	1	1	20	1	88
5	0.33	1	1	40	1	94
6	0.33	1	1	60	1	98
7	0.33	1	2	80	0.5	>99 (86% ^d)

^aConditions (unless otherwise stated): feed 1, 1 M **4** in AcOH; feed 2, 15 M HNO₃ in H₂O; feed 1/feed 2 flow rate ratio = 1:2, corresponding to 30 equiv of HNO₃. ^bFeed 1/feed 2 flow rate ratio = 1:1, corresponding to 15 equiv of HNO₃. ^cYields based on area % measured with UHPLC. Regioisomer **6** was not observed. ^dIsolated yield after recrystallization.

Scheme 3. Flow Scheme for the Nitration of **4** to the Nitrated Analogue **5** Using White Fuming Nitric Acid



the reaction feed was reduced to 40 °C, the product crystallized inside the flow reactor, making a dilution to 0.5 M substrate in AcOH necessary. We then screened the influence of the residence time on the yield of product **5** using 4 equiv of fuming HNO₃ (Figure 2). A longer residence time afforded a higher yield but resulted in a lower throughput for a given reactor volume, corresponding to a lower space-time yield.

The previous results demonstrated that the reaction displayed only a weak temperature dependence. We were interested in further investigating the influence of temperature on the reaction performance because a lower temperature resulted in higher yield with fewer oxidation side products, whereas higher reaction temperatures resulted in elevated decomposition. We actively cooled the reactor to 20 °C and tried to improve the conversion again by increasing the number of equivalents of fuming nitric acid used (Figure 3). The flow rate of the substrate (F1) was kept constant at 667 or 333 μL/min. In the case of the lower flow rate (333 μL/min), 10 equiv of HNO₃ was sufficient to obtain full conversion of the starting material within the volume of the FlowPlate. When the higher flow rate (667 μL/min) was used, 16 equiv of HNO₃ was necessary to obtain 98% conversion. These results indicate that a higher yield without noticeable decomposition can be obtained at longer residence times and with a larger number of equivalents of HNO₃.

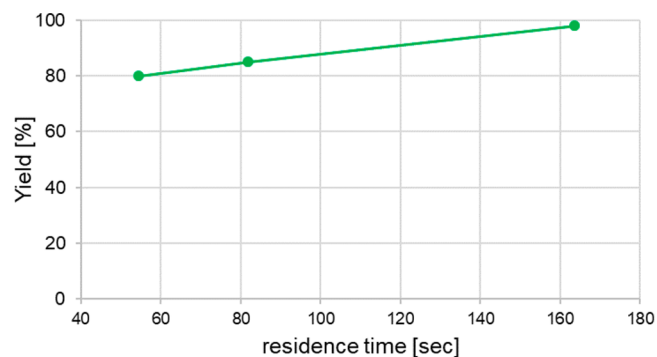


Figure 2. Optimization of the residence time for the nitration of **4** to the nitrated analogue **5** using white fuming nitric acid (4 equiv). Conditions: feed 1, 0.5 M **4** in AcOH; feed 2, fuming nitric acid; feed 1/feed 2 flow rate ratio = 100:9; reaction feed heated to 40 °C. Yields are based on area % measured by HPLC.

Subsequently, we examined the possibility of telescoping the acetylation and nitration steps within a single continuous flow reaction sequence without isolation or purification of intermediate **4** (Scheme 4). The transfer of the first step into flow was especially intriguing since we had observed exothermic behavior during the initial addition of Ac₂O. Moreover, since Ac₂O was used in excess, the formation of potentially explosive acetyl nitrate through reaction with nitric acid could occur. We deemed this safety issue to be manageable because of the very small quantities that would be formed at any one time within the flow reactor.

We achieved the acetylation by pumping **3** dissolved in AcOH (feed 1, flow rate = 666 μL/min, 1 equiv, 0.5 M) and neat Ac₂O (feed 2, flow rate = 40 μL/min, 1.2 equiv) and mixing the two feeds in a T-piece. The reaction solution was then reacted within a residence time unit (PFA, 1/8 in. o.d., 0.8 mm i.d., V = 5 mL) for 7 min before being mixed with fuming nitric acid (feed 3, flow rate = 210 μL/min, 15 equiv) in the FlowPlate. The reaction stream was quenched by introducing the effluent into a stirred 4 M NaOH solution at 0 °C. The product crystallized immediately upon contact with water. The

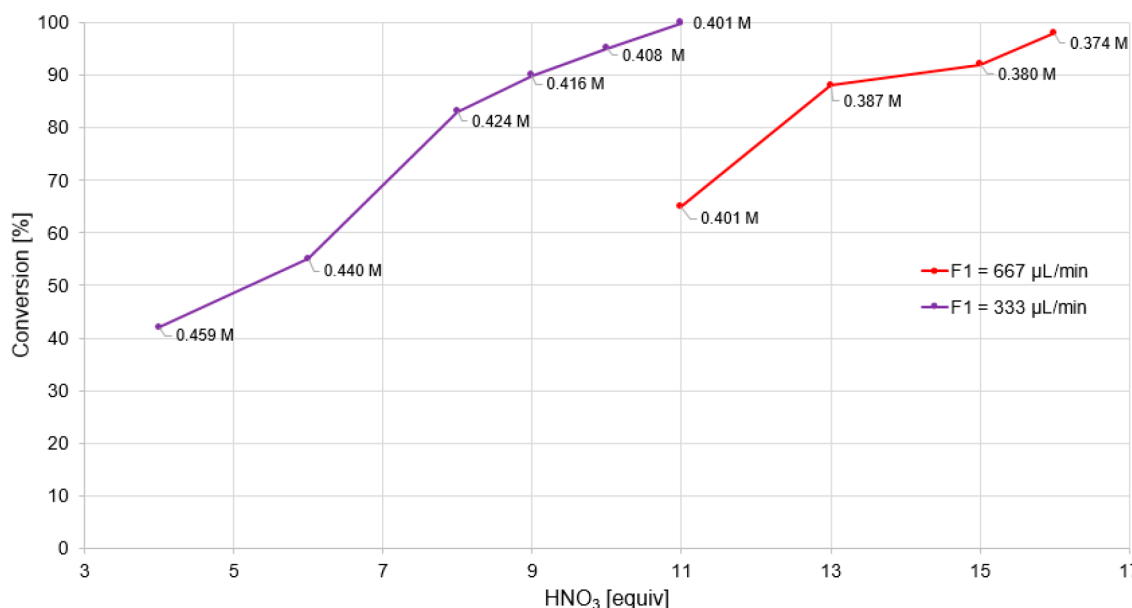
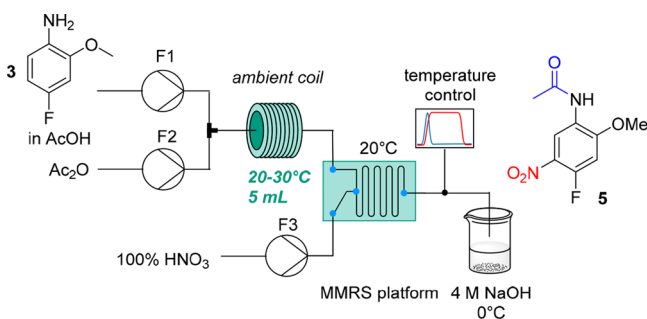


Figure 3. Study to optimize the number of equivalents of white fuming nitric acid in the nitration of **4** in acetic acid. Conditions: feed 1, 0.5 M **4** in AcOH; feed 2, fuming nitric acid; feed 1/feed 2 flow rate ratio = 100:(2.25 × number of equivalents); reaction feed cooled to 20 °C. Concentrations given in the graph correspond to concentration of **4** within the reactor. Yields are based on area % measured by HPLC.

Scheme 4. Flow Scheme for Telescoping of the Acetylation and Nitration^a



^aConditions: feed 1, 0.5 M **4** in AcOH; feed 2, neat Ac₂O; feed 3, fuming nitric acid (99%); flow rates for feed 1/feed 2/feed 3 = 666/40/210 µL/min; reaction feed cooled to 20 °C.

effluent was continuously quenched, which meant that no exotherm was observed. This protocol resulted in 96% conversion with 95% selectivity for compound **5**. The slight improvement in selectivity and yield could be explained by the action of surplus Ac₂O (0.2 equiv) as a water scavenger. Removal of the water drives the reaction equilibrium toward the desired product side.

B. Mass-Transfer-Limited Nitration. In order to further reduce the salt waste, increase the space-time yield, and create an in situ water scavenger to avoid product precipitation during the reaction (from water formation), we needed to further reduce the amount of nitric acid used by employing an even more reactive nitration system. To achieve this goal, we used fuming sulfuric acid (H₂SO₄ + 18 wt % SO₃) as a water scavenger and catalyst to enhance the reaction rate of the nitration (Table 2). The optimization to determine the lowest possible HNO₃ input was achieved by gradually increasing the amount of fuming H₂SO₄ and decreasing the amount of nitric acid used (Table 2, entries 1–5). In the case of 1.15 equiv of fuming nitric acid (entries 4 and 5), very low flow rates of

nitric and sulfuric acid were used (20 µL/min for HNO₃ and 10 µL/min for H₂SO₄). If there were a drop in either acid feed due to process deviation, then a drop in selectivity for the desired isomer **5** would likely be observed. To ensure reliable results in these cases we had to account for very small fluctuations in the flow rates caused by the switch valves in the syringe pump heads. We solved this issue through the installation of a residence time loop with a volume of 4 mL after the FlowPlate to enable a longer residence time in order to complete the reactor macromixing. In section A this was not an issue since the nitric acid was used in a larger excess, so small deviations would have only a minor influence on the results. Furthermore, we increased the flow rate for feed 1 to 1 mL/min to allow increases in the flow rates of HNO₃ and H₂SO₄ accordingly. We anticipated that the residence time unit after the FlowPlate would not be necessary during operation at larger scale because the higher flow rates used and more precise pumps (e.g., gear pumps) would provide more controlled dosing of the reagents.

To demonstrate the stability of our optimized process, a long-run experiment was conducted over 80 min of operation time (Scheme 5). Since the ratio of HNO₃ to oleum did not need to be changed, as in the optimization experiments, we decided to premix the two acids in a 1:1 molar ratio and introduce the feed solution with one pump. The mixing of the two fuming acids generated a small exotherm, and thus, careful addition was necessary. The acid mixture can be safely stored and is not fuming, making it easier to handle than fuming H₂SO₄ and fuming HNO₃. The process was stable throughout the duration of the run. The long run afforded **5** in 82% isolated yield (7.4 g) with >99% purity by HPLC after recrystallization, corresponding to a throughput of 5.6 g/h (25 mmol/h).

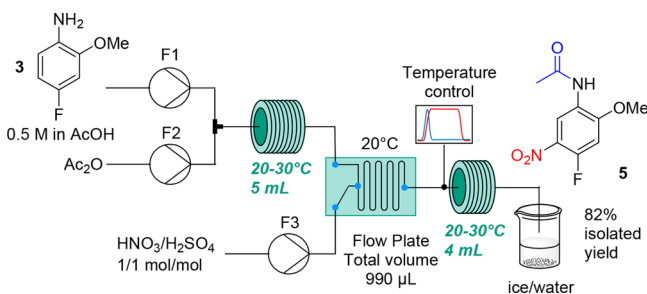
In order to obtain the desired API intermediate **2**, crystalline **5** was suspended in 0.7 M aqueous HCl to perform the deacetylation. The suspension was heated to 76 °C, which resulted in dissolution of all solids. After heating for 5 h, full conversion of starting material was observed by HPLC. A

Table 2. Optimization of Fuming Sulfuric Acid Input for the Nitration of 4 to Achieve Minimal HNO₃ Input^a

entry	equiv of fuming H ₂ SO ₄	yield of 5 [%] ^b		
		3 equiv of HNO ₃	2 equiv of HNO ₃	1.15 equiv of HNO ₃
1	0.15	92	39	—
2	0.30	99	90	—
3	0.50	—	99	—
4	0.70	—	—	92 ^c
5	1.15	—	—	99 ^c

^aConditions (unless otherwise stated): feed 1, 0.5 M 3 in AcOH; feed 2, neat Ac₂O; feed 1/feed 2 flow rate ratio = 100:6; feed 3, fuming HNO₃; feed 4, fuming H₂SO₄ (H₂SO₄ + 18 wt % SO₃). ^bBased on area % measured by HPLC and confirmed by NMR spectroscopy. Full conversion of the starting material 3 was observed in all of the experiments. ^cF1 was 1 mL/min, and a 4 mL residence time unit was used after the FlowPlate.

Scheme 5. Continuous Flow Setup for the Long-Run Experiment^a



^aFeed 1, 0.5 M 3 in AcOH; feed 2, neat Ac₂O; feed 3, 1:1 mol/mol fuming HNO₃/fuming H₂SO₄. Flow rates: F1/F2/F3 = 1000/60/49 µL/min.

simple extraction protocol using aqueous NaHCO₃/MTBE followed by filtration and drying afforded the product in 97% isolated yield. Direct telescoping of the deprotection within a continuous flow environment was not attempted because the deprotection requires aqueous acid, which causes precipitation of the protected compound 5. Thus, we chose to perform the deprotection under batch conditions.

C. Scale-Up. The laboratory procedure based on the smaller FlowPlate Lab of size 600 was then transferred to Lonza (Visp, Switzerland) for scale-up implementation (Table 3). The size of 600 corresponds to the mixing unit size at the

Table 3. Mixing Unit Size at Smallest Cross-Sectional Area and Nominal Flow Rates²⁴

size	d_h [mm]	width [mm]	depth [mm]	nominal flow rates [mL/min]	scaling factor
600 (lab)	0.286	0.20	0.50	1.5–15	1
300	0.714	0.50	1.25	15–150	10

smallest cross-sectional area. For this purpose, the FlowPlate A6/A5 reactor technology was used (Figure 4), which is based on a multiscale approach wherein plates of different sizes are used and adapted to the reaction requirements.¹⁹ The larger plates (A6 and A5) are individual Hastelloy-made plates that are sandwiched between highly thermally conductive aluminum or copper plates for thermal fluid passage. The overall reactor can sustain pressures of up to 100 bar. The main advantage of this reactor technology is its facile scalability. Figure 4 shows the reactor designs that were developed to allow operation over a wide range of flow rates (1.5 up to 600 mL/min) and scales. Detailed information regarding the mixer sizes has been described elsewhere.²⁴

Since nitration reactions using concentrated sulfuric acid are often very fast and highly exothermic, it is important to ensure efficient mixing and heat transfer. In addition, a short time can be necessary for the acid stream (in this case HNO₃/H₂SO₄/SO₃) and the organic stream to become a single phase within the reactor. One of the main objectives for scale-up of a mass-transfer-limited and exothermic reaction to production scale is to keep the dimensionless Damköhler numbers for heat and mass transfer as constant as possible.²⁵ The Damköhler numbers relate the chemical reaction time scale to the transport phenomena rate occurring in a system. One strategy to achieve this during scale-up is through a smart dimensioning approach. Mixing behavior can be predicted and compared to a flow regime map to identify the appropriate reactor module design. An A5-sized LL-rhombus-type micromixer (11 mL mixing plate, channel width 0.5 mm, channel depth 1.25 mm) designed for liquid/liquid applications has been shown to be more effective than classical sinusoidal mixers for this type of nitration (Figure 5). At the proper flow rate, it ensures a drop/dispersed-flow regime often with turbulent flow and therefore efficient heat and mass transfer throughout the entire plate.^{21e} The A5 plate is ca. 4 times the size of the FlowPlate Lab and can process up to 150 mL/min with mixing elements of size

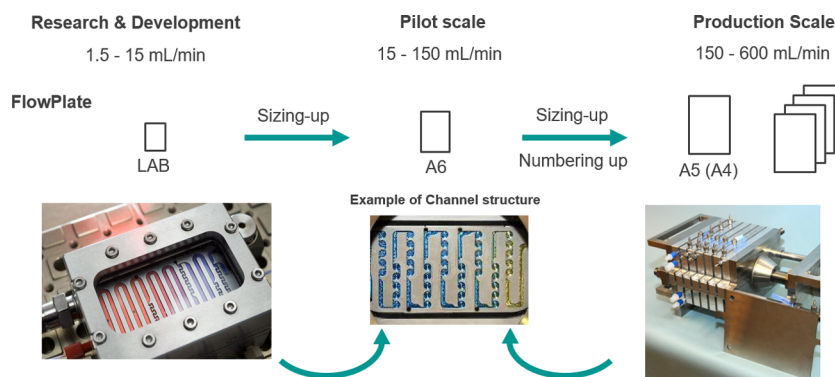


Figure 4. Plate scale-up concept based on the multiscale approach.

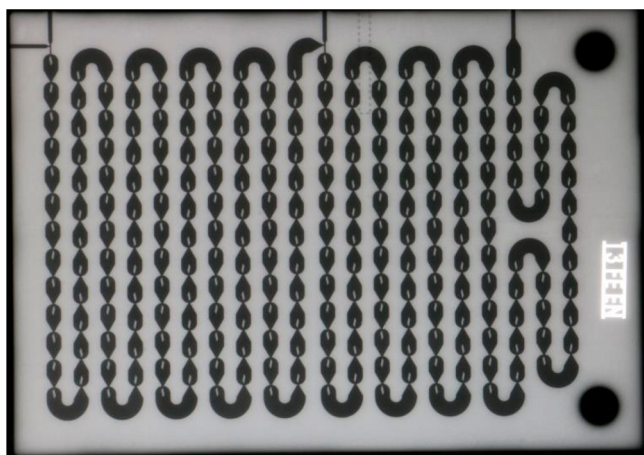


Figure 5. X-ray picture of a FlowPlate A5 reactor plate with geometrically equivalent LL mixers of size 300 from Figure 4 for higher flow rates. The surface area of the plate is 148 mm × 210 mm.

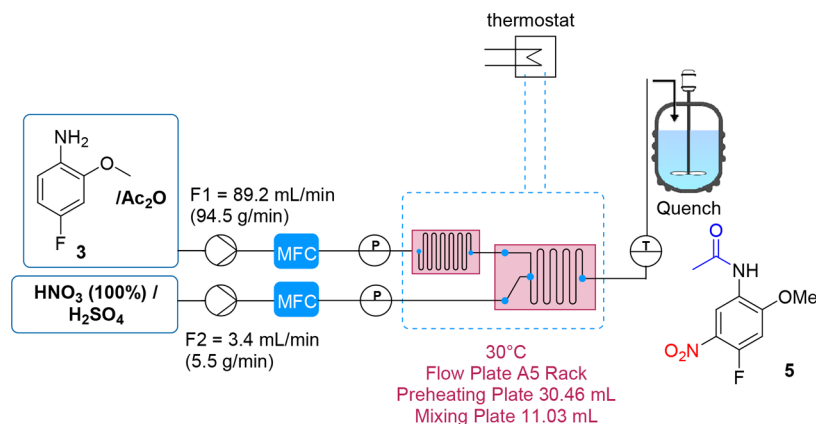
300.^{21a} The scale-up to the A5 rack was based on sizing up the channel dimensions, and thus, it was designed to be geometrically equivalent to the lab version, giving a similar mixing efficiency at a higher flow rate while still ensuring high heat removal capacity as further described below.

The reactor configuration consisted of two pumps, each equipped with a mass flow controller (MFC) (Scheme 6). The fastest-flowing feed passed through a preheater plate (30 mL) at 30 °C and then was mixed with the second feed within an A5-sized LL-rhombus-type micromixer (size 300) at 30 °C.

The effluent from the flow reactor was quenched into a vessel containing water. A residence time loop after the reactor was no longer necessary for the scale-up because of better control over pumping of the feeds. The results from the laboratory-scale experiments (Table 2) could be reproduced. Feed 1 consisted of 6.5 wt % **3** (0.45 M), 9.5 wt % Ac₂O (0.54 M, 1.2 equiv), and 84 wt % AcOH to closely resemble our small-scale conditions. Feed 2 consisted of fuming HNO₃/oleum (1.1 equiv of HNO₃, 1:1 w/w). It was found that the entire exotherm could be controlled within a single plate (Figure 6), highlighting the enhanced heat transfer capacities of this reactor technology. Intermediate **5** precipitated in the quench. The process afforded the acetylated and nitrated compound **5** in 83% yield (76.4 g) with >99% purity after filtration and drying. Thus, a throughput of 2 mol/h could be achieved, corresponding to a scale-up factor of 70.

After successful implementation of the lab-scale conditions at a pilot scale, we were then interested in further fine-tuning of the operating conditions within the FlowPlate A5. Increasing the amount of acetic anhydride to 2.0 molar equiv relative to **3** in further experiments resulted in higher solubility, keeping the reactants and products in solution even when the initial concentration of **3** in feed 1 was increased from 1.1 to 1.7 M. Furthermore, H₂SO₄ and 2 equiv of Ac₂O were sufficient to act as a water scavenger. Thus, the use of oleum was no longer necessary. The isolated yield of *N*-(4-fluoro-2-methoxy-5-nitrophenyl)acetamide (**5**) increased at higher flow rates (Figure 7), indicating that the nitration reaction in the A5-sized LL-rhombus FlowPlate is mass-transfer-limited. Better mixing could be achieved by using higher flow rates. This trend

Scheme 6. Continuous Flow Setup for the Scale-Up in a FlowPlate A5 Rack with an 11 mL LL Mixing Plate



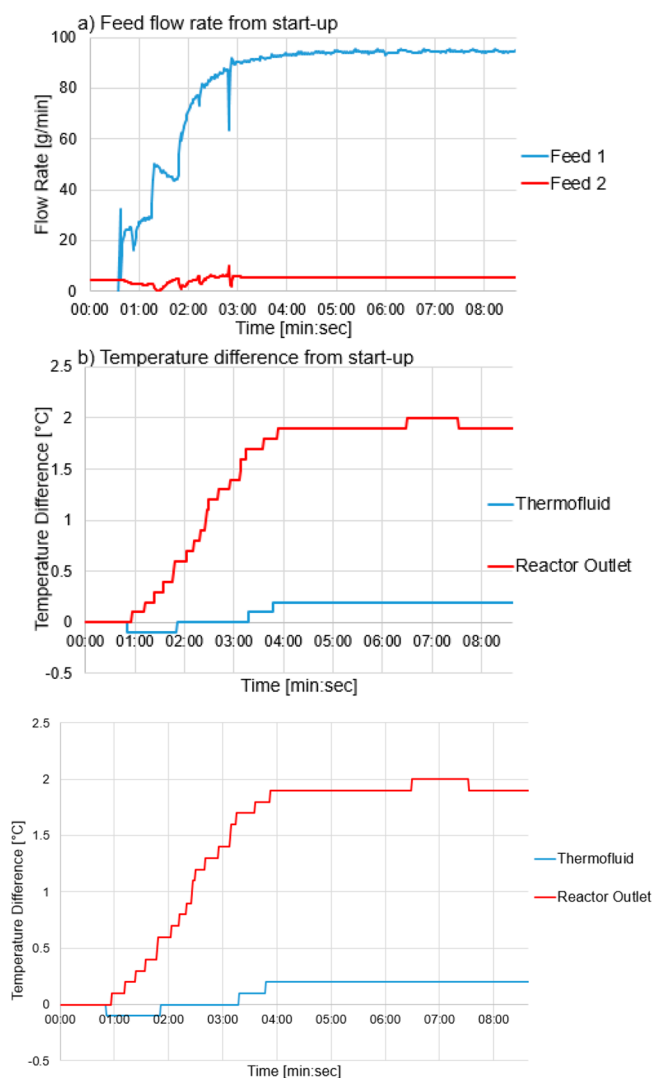


Figure 6. Continuous flow experiment using the A5-sized LL-rhombus FlowPlate. Feed 1, 6 wt % **3** (0.45 M) and 5.2 wt % Ac₂O (0.54 M, 1.2 equiv) in AcOH; feed 2, 1:1 w/w fuming HNO₃/oleum. Flow rates: F1 = 89.2 mL/min = 94.5 g/min; F2 = 3.4 mL/min = 5.5 g/min. The volume of the mixing reactor was 11 mL. When the two feeds were switched on, an exotherm was observed since the reactor outlet temperature increased. The fact that the reactor outlet temperature was stable showed that the entire exotherm could be controlled within a single plate, highlighting the enhanced heat transfer capacities of the reactor technology.

could be observed for both initial concentrations of **3** in feed 1 (1.1 and 1.7 M). Operation at a higher concentration enables an increase in productivity for the flow process. The nitration temperature showed no significant influence on the purity and isolated yield of **5** between 20 and 40 °C (Figure 8). The absence of a temperature dependence is another indication that the nitration reaction in the A5-sized LL-rhombus FlowPlate is fully mass-transfer-limited.

The possibility of full commercial implementation under the optimized conditions (feed 1 = 1.1 M **3** and 2.2 M Ac₂O in AcOH; feed 2 = 1.3 equiv (30 wt %) HNO₃ in H₂SO₄; residence time = 7.8 s) was then considered to evaluate scale-up for a campaign requiring production of 3500 kg of **2**. The calculations were based on the conditions producing **5** in 83% yield. For a campaign duration of 35 days and a productivity of 100 kg/day, flow rates of 392.1 g/min for feed 1 and 98.6 g/

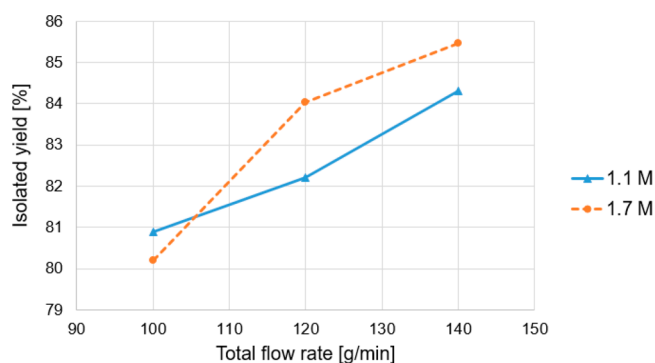


Figure 7. Influence of the flow rate measured for two different concentrations of **3**, with feed 1 containing 1.1 M **3** (13 wt %) and Ac₂O (18.8 wt %, 2 equiv) (blue curve) or 1.7 M **3** (18 wt %) and Ac₂O (26.1 wt %, 2 equiv) (orange curve). Feed 2 was 30:70 w/w fuming HNO₃/H₂SO₄, and the feed 1/feed 2 flow rate ratio was 7.73:1 (1.3 equiv of HNO₃). The mixing reactor volume was 11 mL.

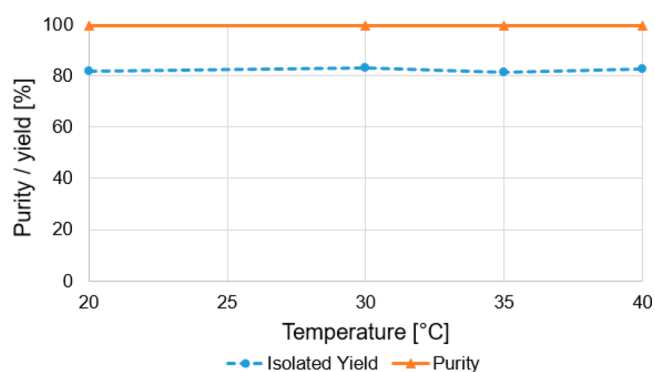


Figure 8. Influence of the temperature on the yield and purity. Feed 1 contained 1.1 M **3** (13 wt %), AcOH (13 wt %), and Ac₂O (18.8 wt %, 2 equiv). Feed 2 was 30:70 w/w fuming HNO₃/H₂SO₄. The feed 1/feed 2 flow rate ratio was 7.73:1 (1.3 equiv of HNO₃). The mixing reactor volume was 11 mL.

min for feed 2 would have to be used. For example, an A5-sized LL-rhombus-type mixer can be used by placing four mixing plates with larger channel dimensions than before (channel width 0.7 mm, channel depth 1.75 mm; size 200) in series to achieve a similar performance as in the pilot-scale study. Running under these conditions corresponded to a theoretical space-time yield of 1923 kg L⁻¹ day⁻¹. The highly exothermic quench of the reaction solution could then possibly be achieved by feeding the reactor effluent while simultaneously introducing a water feed into a continuously stirred tank reactor (CSTR).

CONCLUSION

We have described the development and scale-up of a continuous flow protocol for the preparation of *N*-(4-fluoro-2-methoxy-5-nitrophenyl)acetamide by a two-step telescoped acetylation/nitration. Subsequent batch deprotection afforded 4-fluoro-2-methoxy-5-nitroaniline, an important precursor in the manufacture of osimertinib. Three different nitration strategies were evaluated with regard to their overall productivity and scalability. We optimized the nitration reaction using AcOH/aqueous HNO₃, AcOH/100% HNO₃, and finally 100% HNO₃/fuming H₂SO₄. The acetylation and nitration could be successfully telescoped, and the telescoped process was operated for 80 min to afford the target molecule

in 82% isolated yield over two steps, corresponding to a throughput of 25 mmol/h. Deacetylation could be achieved under batch conditions by using dilute HCl to afford the desired building block 4-fluoro-2-methoxy-5-nitroaniline in 97% yield. The developed process was successfully transferred from laboratory to pilot scale by using a larger-scale flow reactor to enable pilot-scale studies. The throughput was increased to 2 mol/h in the Lonza FlowPlate AS rack by increasing the flow rates and substrate concentration. The product was isolated in 83% yield with >99% purity after filtration and drying, demonstrating very good transfer of the laboratory-scale conditions. The reaction exotherm for the nitration was controlled within a single plate at both the laboratory and pilot scale. The flow protocol described herein significantly improves the yield and process safety compared with the previously reported batch protocols for this nitration. Possible commercial manufacturing conditions based on the laboratory- and pilot-scale results were considered.

EXPERIMENTAL SECTION

General. ^1H NMR spectra were recorded on a Bruker 300 MHz instrument. ^{13}C NMR spectra were recorded on the 300 MHz instrument at 75 MHz. ^{19}F NMR spectra were recorded on the 300 MHz instrument at 282 MHz. Chemical shifts (δ) are expressed in parts per million downfield from tetramethylsilane as an internal standard. The letters s, d, dd, t, q, and m are used to indicate singlet, doublet, doublet of doublets, triplet, quadruplet, and multiplet. The purity and supplier for each chemical were the following: 4-fluoro-2-methoxyaniline (**3**) (98% purity, Fluorochem); acetic anhydride ($\geq 99\%$ purity, VWR); acetic acid ($\geq 99\%$ purity, VWR); HNO_3 (99 wt %, Lonza AG); sulfuric acid ($\geq 99\%$ purity, +19 wt % SO_3 , Sigma-Aldrich); concentrated HCl (35% in water, VWR); dichloromethane (>98% purity, VWR). Microwave reactions were performed using a Biotage Initiator+ single-mode microwave instrument. Reaction times refer to hold times at the temperatures indicated and not to total irradiation times. The temperature was measured with an IR sensor on the outside of the reaction vessel.

Notice of Caution. Mixtures of Ac_2O with HNO_3 or especially $\text{HNO}_3/\text{H}_2\text{SO}_4$ can form highly explosive acetyl nitrate (AcNO_3).²⁶ It is highly recommended that a proper risk assessment be performed and precautions be taken before the reactions described in this article are performed. Fuming nitric and sulfuric acid are highly caustic toward human skin. Wearing personal protective equipment, including safety goggles, Vitoject gloves, and a lab coat, is recommended.

Telescoped Continuous-Flow Acetylation and Nitration of 4-Fluoro-2-methoxyaniline (3**) to Give *N*-(4-Fluoro-2-methoxy-5-nitrophenyl)acetamide (**5**).** The flow setup consisted of three continuous syringe pumps ($3 \times$ Asia Syrris) to introduce a solution of **3** in acetic acid (AcOH) (feed 1), acetic anhydride (Ac_2O) (feed 2), and an acid mixture of fuming $\text{HNO}_3/\text{oleum}$ (1:1 mol/mol) (feed 3). Feeds 1, 2, and 3 were directly pumped using syringe pumps. Before the experiment commenced, the reactor setup was flushed by pumping neat AcOH at a flow rate of 1000 $\mu\text{L}/\text{min}$ using the pump for feed 1. Subsequently, Ac_2O (feed 2) was introduced into the flow system at a flow rate of 60 $\mu\text{L}/\text{min}$ (1.2 equiv), and the acid mixture (feed 3) was introduced at a flow rate of 50 $\mu\text{L}/\text{min}$ (1.25 equiv). **3** (7.06 g, 50.0 mmol) was diluted to 100 mL with AcOH in a volumetric flask to prepare feed 1. To commence the experiment, pump 1 was

switched from neat AcOH to feed 1 while the flow rate was maintained at 1000 $\mu\text{L}/\text{min}$. Feeds 1 and 2 were combined within a Y-shaped connector (Y Assembly PEEK $1/4$ -28, 0.040 in) at ambient temperature. The combined mixture was passed through a reactor coil (PFA, $1/8$ in. o.d., 0.8 mm i.d., residence volume $V_1 = 5.0$ mL) at ambient temperature and then through an inlet (Ehrfeld MMRS, Fitok $1/16$ in. HC, volume $V_2 = 410$ μL) before being combined with the acid mixture within a microreactor (Ehrfeld FlowPlate Lab Microreactor HC, process plate LL, channel width = 2 mm, mixer nominal width = 0.2 mm, volume $V_3 = 0.4$ mL). The FlowPlate was cooled to 20 $^\circ\text{C}$ using a thermostat (Huber CC 304, 4000 rpm, water-cooled). After the FlowPlate, the reaction mixture was passed through a temperature sensor (Ehrfeld Xyfluor 0501-1; volume $V_4 = 165$ μL), an outlet (Ehrfeld MMRS, Fitok $1/16$ in. HC, volume $V_5 = 410$ μL), and a reactor coil (PFA, $1/8$ in. o.d., 0.8 mm i.d., volume $V_6 = 4.0$ mL) at 20 $^\circ\text{C}$. The output solution was diluted with an ice/water mixture (1:1 v/v). The effluent was collected over 80 min (corresponding to 40 mmol of material) and extracted with EtOAc (3×100 mL). The combined organic phases were dried over Na_2SO_4 , filtered, and concentrated under reduced pressure. The crude product was dissolved in hot MeCN and treated with H_2O until precipitation was observed. The resulting slurry was heated to reflux until all of the solids were dissolved and then cooled to 4 $^\circ\text{C}$ for 3 h. The obtained crystals were filtered and washed with cold MeCN and H_2O to afford **5** (7.49 g, 32.8 mmol, 82% yield) as colorless crystals. Mp 226–227 $^\circ\text{C}$; ^1H NMR (300.36 MHz, $\text{DMSO}-d_6$) δ 9.53 (s, 1H), 8.86 (d, $^3J_{\text{HF}} = 8.2$ Hz, 1H), 7.30 (d, $^3J_{\text{HF}} = 13.3$ Hz, 1H), 3.98 (s, 3H), 2.12 (s, 3H); ^{13}C NMR (75 MHz, $\text{DMSO}-d_6$) δ 169.2, 155.5 (d, $^2J_{\text{CF}} = 10.0$ Hz), 152.7 (d, $^1J_{\text{CF}} = 260.7$ Hz), 128.3, 124.1, 117.5, 101.4 (d, $^2J_{\text{CF}} = 26.1$ Hz), 57.3, 23.8; ^{19}F NMR (282 MHz, $\text{DMSO}-d_6$) δ -118.8 (dd, $^3J_{\text{HF}} = 12.5$ Hz, $^3J_{\text{HF}} = 9.1$ Hz).

Synthesis of *N*-(4-Fluoro-2-methoxyphenyl)acetamide (4**).** A round-bottom flask equipped with a stir bar was charged with **3** (1.41 g, 10.0 mmol). Ac_2O (2.04 g, 20.0 mmol) was slowly added to the vigorously stirred substrate. A light-pink precipitate was formed, which was filtered and washed with H_2O . The crude product was recrystallized from MeCN to give **4** as light-pink crystals (1.76 g, 9.58 mmol, 96% yield). Mp 139–140 $^\circ\text{C}$; ^1H NMR (300.36 MHz, CDCl_3) δ 8.27 (dd, $^3J_{\text{HH}} = 8.8$ Hz, $^4J_{\text{HF}} = 6.2$ Hz, 1H), 7.59 (s, 1H), 6.69–6.56 (m, 2H), 3.85 (s, 3H), 2.18 (s, 3H); ^{13}C NMR (75 MHz, CDCl_3) δ 168.2, 159.2 (d, $^1J_{\text{CF}} = 242.6$ Hz), 148.95 (d, $^3J_{\text{CF}} = 9.8$ Hz), 123.90 (d, $^4J_{\text{CF}} = 3.1$ Hz), 120.76 (d, $^3J_{\text{CF}} = 9.1$ Hz), 106.80 (d, $^2J_{\text{CF}} = 21.5$ Hz), 98.74 (d, $^2J_{\text{CF}} = 27.2$ Hz), 56.01, 24.86; ^{19}F NMR (282 MHz, CDCl_3) δ -116.64 (ddd, $^3J_{\text{HF}} = 9.8$ Hz, $^3J_{\text{HF}} = 8.4$ Hz, $^4J_{\text{HF}} = 6.3$ Hz).

Synthesis of 4-Fluoro-2-methoxy-5-nitroaniline (2**) (Deprotection).** To a three-neck round-bottom flask was added **5** (1.01 g, 4.37 mmol) suspended in EtOH (21.63 mL). Aqueous HCl (26%, 2.17 mL, 1.75 mmol) was slowly added to the suspension over 5 min ($T < 30$ $^\circ\text{C}$). After addition, the mixture was warmed to 83 $^\circ\text{C}$ ($T_{\text{inside}} = 76$ $^\circ\text{C}$) and stirred for 5 h at this temperature. The solvent was removed under reduced pressure (40 $^\circ\text{C}$, 150–40 mbar), and a beige crude product was obtained. Subsequently the crude product was suspended in MTBE (25 mL), and a saturated aqueous solution of NaHCO_3 (25 mL) was added. The two phases were separated, and the aqueous layer was extracted with MTBE (2×25 mL). The combined organic layers were

washed with a saturated aqueous solution of NaCl (10 mL), and after separation of the two phases, the organic phase was concentrated under reduced pressure (40 °C, 350–40 mbar). The desired product **2** was obtained as an orange solid (795 mg, 97% yield). ¹H NMR (400.13 MHz, DMSO-*d*₆) δ 7.36 (d, *J* = 7.91 Hz, 1H), 7.03 (d, *J* = 13.3 Hz, 1H), 5.24 (s, 2H), 3.93 (s, 3H); ¹⁹F NMR (282 MHz, CDCl₃) δ -125.34 (dd, *J* = 12.4, 7.2 Hz).

Scaled-Up Synthesis of 5. The flow setup consisted of two pumps (pump 1 = Fuji HYM-PG-08_12M_Hastelloy; pump 2 = HNP mzx-7255) controlled by mass flow controllers (Coriolis Endress Hauser) via a feedback loop. Pump 1 was used to introduce feed 1 consisting of **3** (0.45 M, 6 wt %, 1 equiv) and Ac₂O (0.54 M, 5.2 wt %, 1.2 equiv) in AcOH. Pump 2 was used to introduce feed 2 consisting of fuming HNO₃/oleum (1.1 equiv of HNO₃, 1:1 w/w). The reactor was washed with AcOH before the experiment was started. To commence the experiment, the two feeds were switched on simultaneously. Feed 1 was directly pumped through pump 1 at a flow rate of 94.5 g/min (89.2 mL/min). Feed 1 was preheated to 30 °C in a preheating plate within the A5 FlowPlate rack (*V*_{preheat} = 30.46 mL). Feed 2 was directly pumped through pump 2 at a flow rate of 5.5 g/min (3.4 mL/min). Feed 1 and feed 2 were introduced into a FlowPlate A5 (*V*_{reactor} = 11.03 mL), where feed 2 was mixed with the preheated feed 1. After exiting the mixing plate, the reaction feed was collected for 10 min within a stirred tank reactor containing 4 times the amount of water in relation to the expected reaction feed. Immediate precipitation occurred after contact with water, resulting in the formation of a beige solid. The precipitated solid was filtered, washed with 1 volume of water, and dried in a vacuum oven to afford **5** (76.4 g, 0.335 mol, 83% yield) as a beige crystalline solid.

■ ASSOCIATED CONTENT

Supporting Information

The Supporting Information is available free of charge at <https://pubs.acs.org/doi/10.1021/acs.oprd.0c00254>.

Full experimental details, description and images of the continuous flow setup, and ¹H, ¹⁹F, and ¹³C NMR spectra of all isolated products (PDF)

■ AUTHOR INFORMATION

Corresponding Authors

Christopher A. Hone – Center for Continuous Flow Synthesis and Processing (CCFLOW), Research Center Pharmaceutical Engineering GmbH (RCPE), A-8010 Graz, Austria; Institute of Chemistry, University of Graz, A-8010 Graz, Austria;

orcid.org/0000-0002-5939-920X;

Email: christopher.hone@rcpe.at

C. Oliver Kappe – Center for Continuous Flow Synthesis and Processing (CCFLOW), Research Center Pharmaceutical Engineering GmbH (RCPE), A-8010 Graz, Austria; Institute of Chemistry, University of Graz, A-8010 Graz, Austria;

orcid.org/0000-0003-2983-6007; Email: oliver.kappe@uni-graz.at

Authors

Manuel Köckinger – Center for Continuous Flow Synthesis and Processing (CCFLOW), Research Center Pharmaceutical Engineering GmbH (RCPE), A-8010 Graz, Austria; Institute of Chemistry, University of Graz, A-8010 Graz, Austria

Benjamin Wyler – Microreactor Technology, Lonza AG, CH-3930 Visp, Switzerland

Christof Aellig – Microreactor Technology, Lonza AG, CH-3930 Visp, Switzerland

Dominique M. Roberge – Microreactor Technology, Lonza AG, CH-3930 Visp, Switzerland

Complete contact information is available at:

<https://pubs.acs.org/10.1021/acs.oprd.0c00254>

Notes

The authors declare no competing financial interest.

■ ACKNOWLEDGMENTS

The CCFLOW Project (Austrian Research Promotion Agency FFG 862766) is funded through the Austrian COMET Program by the Austrian Federal Ministry of Transport, Innovation and Technology (BMVIT), the Austrian Federal Ministry of Digital and Economic Affairs (BMDW), and the State of Styria (Styrian Funding Agency SFG).

■ REFERENCES

- (1) (a) Finlay, M. R. V.; Anderton, M.; Ashton, S.; Ballard, P.; Bethel, P. A.; Box, M. R.; Bradbury, R. H.; Brown, S. J.; Butterworth, S.; Campbell, A.; et al. Discovery of a Potent and Selective EGFR Inhibitor (AZD9291) of Both Sensitizing and T790M Resistance Mutations That Spares the Wild Type Form of the Receptor. *J. Med. Chem.* **2014**, *57*, 8249–8267. (b) Cross, D. A. E.; Ashton, S. E.; Ghiorghiu, S.; Eberlein, C.; Nebhan, C. A.; Spitzler, P. J.; Orme, J. P.; Finlay, M. R. V.; Ward, R. A.; Mellor, M. J.; Hughes, G.; Rahi, A.; Jacobs, V. N.; Brewer, M. R.; Ichihara, E.; Sun, J.; Jin, H.; Ballard, P.; Al-Kadhimi, K.; Rowlinson, R.; Klinowska, T.; Richmond, G. H. P.; Cantarini, M.; Kim, D.-W.; Ranson, M. R.; Pao, W. *Cancer Discovery* **2014**, *4*, 1046–1061.
- (2) (a) Tan, C.-S.; Gilligan, D.; Pacey, S. Treatment Approaches for EGFR-Inhibitor-Resistant Patients with Non-Small-Cell Lung Cancer. *Lancet Oncol.* **2015**, *16*, e447–e459. (b) Ayeni, D.; Politi, K.; Goldberg, S. B. Emerging Agents and New Mutations in EGFR-Mutant Lung Cancer. *Clin. Cancer Res.* **2015**, *21*, 3818–3820.
- (3) Ramalingam, S. S.; Vansteenkiste, J.; Planchard, D.; Cho, B. C.; Gray, J. E.; Ohe, Y.; Zhou, C.; Reungwetwattana, T.; Cheng, Y.; Chewaskulyong, B.; Shah, R.; Cobo, M.; Lee, K. H.; Cheema, P.; Tiseo, M.; John, T.; Lin, M.-C.; Imamura, F.; Kurata, T.; Todd, A.; Hodge, R.; Saggese, M.; Rukazenkov, Y.; Soria, J.-C. *N. Engl. J. Med.* **2020**, *382*, 41–50.
- (4) (a) Xu, M.; Xie, Y.; Ni, S.; Liu, H. The Latest Therapeutic Strategies after Resistance to First Generation Epidermal Growth Factor Receptor Tyrosine Kinase Inhibitors (EGFR TKIs) in Patients with Non-Small Cell Lung Cancer (NSCLC). *Ann. Transl. Med.* **2015**, *3*, 96–102. (b) Arcila, M. E.; Oxnard, G. R.; Nafa, K.; Riely, G. J.; Solomon, S. B.; Zakowski, M. F.; Kris, M. G.; Pao, W.; Miller, V. A.; Ladanyi, M. *Clin. Cancer Res.* **2011**, *17*, 1169–1180. (c) Sun, J.-M.; Ahn, M.-J.; Choi, Y.-L.; Ahn, J. S.; Park, K. *Lung Cancer* **2013**, *82*, 294–298. (d) Kuiper, J. L.; Heideman, D. A. M.; Thunnissen, E.; Paul, M. A.; van Wijk, A. W.; Postmus, P. E.; Smit, E. F. Incidence of T790M mutation in (sequential) rebiopsies in EGFR-mutated NSCLC-patients. *Lung Cancer* **2014**, *85*, 19–24. (e) Li, W.; Ren, S.; Li, J.; Li, A.; Fan, L.; Li, X.; Zhao, C.; He, Y.; Gao, G.; Chen, X.; Li, S.; Shi, J.; Zhou, C.; Fei, K.; Schmid-Bindert, G. T790M mutation is associated with better efficacy of treatment beyond progression with EGFR-TKI in advanced NSCLC patients. *Lung Cancer* **2014**, *84*, 295–300. (f) Akamatsu, H.; Delmonte, A.; John, T.; Su, W.-C.; Lee, J.-S.; Chang, G.-C.; Huang, X.; Jenkins, S.; Dearden, S.; Wu, Y.-L. EGFR mutation analysis for prospective patient (pt) selection in AURA3 Phase III trial of osimertinib vs platinum-pemetrexed (plt-pem) in pts with EGFR T790M positive advanced non-small cell lung cancer (NSCLC). *Ann. Oncol.* **2017**, *28* (10), x128.

- (5) Butterworth, S.; Finlay, M. R. V.; Ward, R. A.; Kadambar, K.; Chandrashekar, R. C.; Murrugan, A.; Redfearn, H. 2-(2,4,5-Substituted-Anilino) Pyrimidine Derivatives as EGFR Modulators Useful for Treating Cancer. WO 2013/014448 A1, July 2012.
- (6) Lan, J.; Jiang, T.; Li, D.; Liu, X. EGFR Inhibitor and Pharmaceutically Acceptable Salt and Polymorph Thereof, and Use Thereof. WO 2017016463, February 2017.
- (7) Hughes, D. L. Patent Review of Manufacturing Routes to Oncology Drugs: Carfilzomib, Osimertinib, and Venetoclax. *Org. Process Res. Dev.* **2016**, *20*, 2028–2042.
- (8) (a) Hone, C. A.; Boyd, A.; O’Kearney-McMullan, A.; Bourne, R. A.; Muller, F. L. Definitive Screening Designs for Multistep Kinetic Models in Flow. *React. Chem. Eng.* **2019**, *4*, 1565–1570. (b) Holmes, N.; Akien, G. R.; Blacker, A. J.; Woodward, R. L.; Meadows, R. E.; Bourne, R. A. Self-Optimisation of the Final Stage in the Synthesis of EGFR Kinase Inhibitor AZD9291 Using an Automated Flow Reactor. *React. Chem. Eng.* **2016**, *1*, 366–371.
- (9) Barton, J.; Rogers, R. *Chemical Reaction Hazards: A Guide to Safety*, 2nd ed.; Institution of Chemical Engineers: Rugby, U.K., 1997.
- (10) Brocklehurst, C. E.; Lehmann, H.; La Vecchia, L. Nitration Chemistry in Continuous Flow Using Fuming Nitric Acid in a Commercially Available Flow Reactor. *Org. Process Res. Dev.* **2011**, *15*, 1447–1453.
- (11) Hanson, C.; Kaghzachi, T.; Pratt, M. W. T. Side Reactions During Aromatic Nitration. *ACS Symp. Ser.* **1976**, *22*, 132–155.
- (12) Hartman, R. L.; McMullen, J. P.; Jensen, K. F. Deciding Whether To Go with the Flow: Evaluating the Merits of Flow Reactors for Synthesis. *Angew. Chem., Int. Ed.* **2011**, *50*, 7502–7519.
- (13) (a) Gérardy, R.; Emmanuel, N.; Toupy, T.; Kassin, V.; Tshibalonza, N. N.; Schmitz, M.; Monbaliu, J. M. Continuous Flow Organic Chemistry: Successes and Pitfalls at the Interface with Current Societal Challenges. *Eur. J. Org. Chem.* **2018**, *2018*, 2301–2351. (b) Plutschack, M. B.; Pieber, B.; Gilmore, K.; Seeberger, P. H. The Hitchhiker’s Guide to Flow Chemistry. *Chem. Rev.* **2017**, *117*, 11796–11893. (c) Gutmann, B.; Cantillo, D.; Kappe, C. O. Continuous-Flow Technology - A Tool for the Safe Manufacturing of Active Pharmaceutical Ingredients. *Angew. Chem., Int. Ed.* **2015**, *54*, 6688–6728. (d) Movsisyan, M.; Delbecke, E. I. P.; Berton, J. K. E. T.; Battilocchio, C.; Ley, S. V.; Stevens, C. V. Taming Hazardous Chemistry by Continuous Flow Technology. *Chem. Soc. Rev.* **2016**, *45*, 4892–4928.
- (14) (a) Brennecke, H. M.; Kobe, K. A. Mixed Acid Nitration of Toluene. *Ind. Eng. Chem.* **1956**, *48*, 1298–1304. Also see: (b) Cantillo, D. A Pioneering Early Microreactor Concept for Ultrafast Nitration Reactions - Placing the Seminal Brennecke and Kobe 1956 Contribution into Perspective. *J. Flow Chem.* **2015**, *5*, 195–196.
- (15) For a review, see: Kulkarni, A. A. Continuous Flow Nitration in Miniaturized Devices. *Beilstein J. Org. Chem.* **2014**, *10*, 405–424.
- (16) (a) Ducry, L.; Roberge, D. M. Controlled Autocatalytic Nitration of Phenol in a Microreactor. *Angew. Chem., Int. Ed.* **2005**, *44*, 7972–7975. (b) Panke, G.; Schwalbe, T.; Stirner, W.; Taghavi-Moghadam, S.; Wille, G. A Practical Approach of Continuous Processing to High Energetic Nitration Reactions in Microreactors. *Synthesis* **2003**, 2827–2830. (c) Knapkiewicz, P.; Skowerski, K.; Jaskólska, D. E.; Barbasiewicz, M.; Olszewski, T. K. Nitration Under Continuous Flow Conditions: Convenient Synthesis of 2-Isopropoxy-5-nitrobenzaldehyde, an Important Building Block in the Preparation of Nitro-Substituted Hoveyda–Grubbs Metathesis Catalyst. *Org. Process Res. Dev.* **2012**, *16*, 1430–1435. (d) Peters, J.-G.; Stiehl, J.; Lovis, K. Synthesis of Copanlisib and Its Dihydrochloride Salt. US 10,035,803 B2, July 31, 2018. (e) Peters, J.-G.; Rubenbauer, P.; Gotz, D.; Grossbach, D.; Mais, F.-J.; Schirmer, H.; Stiehl, J.; Lovis, K.; Lender, A.; Seyfried, M.; Sweifel, T.; Marty, M.; Weingartner, G. Synthesis of Copanlisib and Its Dihydrochloride Salt. US 10,494,372 B2, December 3, 2019. (f) Qi, G.; Qiu, X.; Shen, J.; Wu, T.; Xie, W.; Zhao, G. Continuous Flow Production Process of 2-Methyl-5-nitroimidazole. CN 110156694 A, August 23, 2019. (g) Ren, J.; Yang, K.; Li, H. Method for Synthesizing Erlotinib Intermediate with Microchannel Reactor. CN 108358798, August 3, 2018. (h) Gage, J. R.; Guo, X.; Tao, J.; Zheng, C. *Org. Process Res. Dev.* **2012**, *16*, 930–933. (i) Yu, Z.; Lv, Y.; Yu, C.; Su, W. *Org. Process Res. Dev.* **2013**, *17*, 438–442.
- (17) Rakshit, S.; Lakshminarasimhan, T.; Guturi, S.; Kanagavel, K.; Kanusu, U. R.; Niyogi, A. G.; Sidar, S.; Luzung, M. R.; Schmidt, M. A.; Zheng, B.; et al. Nitration Using Fuming HNO₃ in Sulfolane: Synthesis of 6-Nitrovanillin in Flow Mode. *Org. Process Res. Dev.* **2018**, *22*, 391–398.
- (18) (a) Cantillo, D.; Damm, M.; Dallinger, D.; Bauser, M.; Berger, M.; Kappe, C. O. Sequential Nitration/Hydrogenation Protocol for the Synthesis of Triaminophloroglucinol: Safe Generation and Use of an Explosive Intermediate under Continuous-Flow Conditions. *Org. Process Res. Dev.* **2014**, *18*, 1360–1366. (b) Cantillo, D.; Wolf, B.; Goetz, R.; Kappe, C. O. Continuous Flow Synthesis of a Key 1,4-Benzoxazinone Intermediate via a Nitration/Hydrogenation/Cyclization Sequence. *Org. Process Res. Dev.* **2017**, *21*, 125–132.
- (19) (a) Roberge, D. M.; Gottspomer, M.; Eyholzer, M.; Kockmann, N. Industrial Design, Scale-up, and Use of Microreactors. *Chim. Oggi* **2009**, *27*, 8–11. (b) Plouffe, P.; Macchi, A.; Roberge, D. M. From Batch to Continuous Chemical Synthesis—a Toolbox Approach. *Org. Process Res. Dev.* **2014**, *18*, 1286–1294.
- (20) Glasnov, T. N.; Kappe, C. O. The Microwave-to-Flow Paradigm: Translating High-Temperature Batch Microwave Chemistry to Scalable Continuous-Flow Processes. *Chem. - Eur. J.* **2011**, *17*, 11956–11968.
- (21) (a) Plouffe, P.; Roberge, D. M.; Macchi, A. Liquid–Liquid Flow Regimes and Mass Transfer in Various Micro-Reactors. *Chem. Eng. J.* **2016**, *300*, 9–19. (b) Mielke, E.; Roberge, D. M.; Macchi, A. Microreactor Mixing-Unit Design for Fast Liquid–Liquid Reactions. *J. Flow Chem.* **2016**, *6*, 279–287. (c) Elvira, K. S.; i Solvas, X. C.; Wootton, R. C. R.; deMello, A. J. The Past, Present and Potential for Microfluidic Reactor Technology in Chemical Synthesis. *Nat. Chem.* **2013**, *5*, 905–915. (d) Mielke, E.; Plouffe, P.; Koushik, N.; Eyholzer, M.; Gottspomer, M.; Kockmann, N.; Macchi, A.; Roberge, D. M. Local and Overall Heat Transfer of Exothermic Reactions in Microreactor Systems. *React. Chem. Eng.* **2017**, *2*, 763–775. (e) Plouffe, P.; Bittel, M.; Sieber, J.; Roberge, D. M.; Macchi, A. On the Scale-up of Micro-Reactors for Liquid–Liquid Reactions. *Chem. Eng. Sci.* **2016**, *143*, 216–225.
- (22) Sagmeister, P.; Williams, J. D.; Hone, C. A.; Kappe, C. O. Laboratory of the Future: A Modular Flow Platform with Multiple Integrated PAT Tools for Multistep Reactions. *React. Chem. Eng.* **2019**, *4*, 1571–1578. (b) Sagmeister, P.; Poms, J.; Williams, J. D.; Kappe, C. O. Multivariate Analysis of Inline Benchtop NMR Data Enables Rapid Optimization of a Complex Nitration in Flow. *React. Chem. Eng.* **2020**, *5*, 677–684.
- (23) *Chemical Resistance Chart*. Siemens, 2008. <https://www.jaspereng.com/wp-content/uploads/2016/12/SiemensChemical-ResistanceChart.pdf> (accessed 07-22-2019).
- (24) Macchi, A.; Plouffe, P.; Patience, G. S.; Roberge, D. M. Experimental Methods in Chemical Engineering: Micro-Reactors. *Can. J. Chem. Eng.* **2019**, *97*, 2578–2587.
- (25) Kockmann, N.; Gottspomer, M.; Zimmermann, B.; Roberge, D. M. Enabling Continuous-Flow Chemistry in Microstructured Devices for Pharmaceutical and Fine-Chemical Production. *Chem. - Eur. J.* **2008**, *14*, 7470–7477.
- (26) (a) Louw, R. Acetyl Nitrate. In *Encyclopedia of Reagents for Organic Synthesis*; Wiley, 2001. DOI: 10.1002/047084289X.ra032. (b) Bordwell, F. G.; Garbisch, E. W., Jr. Nitrations with Acetyl Nitrate. I. The Nature of the Nitrating Agent and the Mechanism of Reaction with Simple Alkenes. *J. Am. Chem. Soc.* **1960**, *82*, 3588–3598.